planktotrophic forms, probably because populations of nonplanktotrophic species face a higher probability of geographic isolation (*1, 3*). Any geographic setting that promotes the isolation of populations of nonplanktotrophic species but not high dispersal forms, should result in the diversification of nonplanktotrophs at a rate greater than that for high dispersal forms.

The Gulf of Mexico coastal plain was subjected to a number of major shoreline transgressions and regressions during the early Tertiary, possibly as a result of global sea-level changes. Regressive intervals were accompanied by the building of large deltas in southern and eastern Texas and the Louisiana-Mississippi area (*3*). Successive paleogeographic reconstructions (*3*) suggest a pattern whereby nonplanktotrophs and planktotrophs achieved gulf-wide ranges during transgressive intervals when deltas were reduced. The ranges of many of the nonplanktotrophs may have been attenuated by deltas during regressive periods while most of the planktotrophic forms were able to disperse around these barriers.

This process of range-partitioning and speciation can lead to higher numbers of nonplanktotrophs relative to planktotrophs, but it does not explain how a group of species may remain dominated by nonplanktotrophs after the range-dividing mechanism ceased to act. A trend has been noted in the marine invertebrates whereby planktotrophic species give rise to nonplanktotrophs but that the reverse is rarely true (*17–19*). Evidence from the Eocene seems to support a unidirectional trend in developmental change (*16*). Several early Tertiary genera that were exclusively planktotrophic gave rise to nonplanktotrophic species. However, no genus that contained all nonplanktotrophic species gave rise to a planktotrophic form.

Given these two trends—a high rate of diversification for nonplanktotrophs and a unidirectional trend in developmental change—if a situation ever arose where a group became completely nonplanktotrophic, it would remain so, even after pressures prompting rapid nonplanktotrophic speciation were removed. Only allochthonous species of the same taxon, migrating from an area where planktotrophic development had not been lost, would be likely to introduce new planktotrophs (*20*). Differential speciation rates and the relative irreversibility of developmental change are probably not the only processes in action promoting increasing proportions of nonplanktotrophs among neogastropods, but these processes must be taken into account when considering changes in developmental types through time.

THOR A. HANSEN
Department of Geological Sciences, University of Texas, Austin 78712

References and Notes

1. T. Shuto, *Lethaia* **7**, 239 (1974).
2. T. A. Hansen, *Science* **199**, 885 (1978).
3. ———, *Paleobiology* **6**, 193 (1980).
4. D. Jablonski, *Geol. Soc. Am. Abstr. Prog.* **10**, 49 (1978).
5. ——— and R. A. Lutz, in *Skeletal Growth of Aquatic Organisms*, D. C. Rhoads and R. A. Lutz, Eds. (Plenum, New York, 1980), p. 323.
6. G. E. Radwin and J. L. Chamberlain, *San Diego Soc. Nat. Hist. Trans.* **17**, 107 (1973).
7. J. B. Taylor, thesis, University of Hawaii, Honolulu (1975).
8. R. T. Paine, *Ecology* **44**, 63 (1963).
9. Development type was determined from the morphology of the protoconch by the criteria explained in (*3*). Hansen (*3*), also comments on taxonomy and geologic ranges. Out of 188 species that met the criteria (*3*), 128 had specimens that retained a protoconch preserved well enough so that a larval determination could be made. Although recovery percentages vary among families, there is no reason to suspect a difference in recovery rate between the two developmental types. The species analyzed should represent an unbiased sampling of the developmental types of the six families. A stratigraphic chart was divided into five time intervals corresponding to transgressive-regressive cycles for the Gulf Coast. Any species that has some part of its range within a particular interval is counted within that interval. Many species are therefore counted more than once in the tabulation in Fig. 1. No species of Nassariidae and Mitridae were recorded for the early Paleocene and none of Nassariidae in the late Eocene. This reflects on absence of preserved protoconchs and not of the species. There is a conspicuous increase in numbers of species late in the middle Eocene that may be partly due to unusually numerous exposures of the Upper Lisbon and Cook Mountain formations. It is possible that the higher number of exposures has allowed more nonplanktotrophs (with narrower ranges) to be sampled during this interval. It is difficult to assess this factor at present, but even if late middle Eocene data are excluded, the overall trend, as depicted in the cumulative percentages, persists.
10. C. S. Weaver and J. E. duPont, *Delaware Mus. Nat. Hist. Monogr. Ser. 1* (1970).
11. A. G. Smith and J. C. Briden, *Mesozoic and Cenozoic Paleocontinental Maps* (Cambridge Univ. Press, Cambridge, 1977).
12. A. Hallam, *Facies Interpretation and the Stratigraphic Record* (Freeman, San Francisco, 1981).
13. A. Delplanque, J. P. Pointier, A. Kermarrec, *Veliger* **17**, 311 (1975).
14. E. J. Petuch, *ibid.* **18**, 322 (1976).
15. T. M. Spight, *ibid.*, p. 309.
16. T. A. Hansen, *Geol. Soc. Am. Abstr. Prog.* **10**, 415 (1978).
17. R. Strathmann, *Am. Nat.* **108**, 29 (1974).
18. ———, *Evolution* **32**, 894 (1978).
19. ———, *ibid.*, p. 907.
20. This hypothesis does not require all neogastropods to show a uniform trend in developmental change through the Cenozoic. Nonplanktotrophs will increase most dramatically when geographic range-dividing mechanisms are at work. If isolating processes are curtailed, this trend could stop or even reverse itself unless the group has already become totally nonplanktotrophic. The lack of a trend in the Buccinidae suggests that these processes were not pervasive.
21. I thank P. Chambers, N. Gilinsky, J. Lang, R. Linsley, and G. Vermeij for discussion and criticism. Supported by the Geology Foundation of the University of Texas at Austin.

11 March 1982; revised 19 October 1982

Liposomal Blockade of the Reticuloendothelial System: Improved Tumor Imaging with Small Unilamellar Vesicles

Abstract. *The reticuloendothelial system of mice bearing EMT6 tumors was effectively blocked by intravenous injections of small unilamellar vesicles that incorporated a 6-aminomannose derivative of cholesterol in the lipid bilayer. Neutral liposomes loaded with indium-111–nitrilotriacetic acid were then injected. Fifty percent more radioactivity was deposited in tumors of the animals with blocked reticuloendothelial systems than in controls. Twenty-four hours after the injection of radioactive vesicles, well-defined tumor images were observed in whole-body gamma camera scintigraphs. Biodistribution studies showed that tumors from animals with blocked reticuloendothelial systems had more than twice the radioactivity per gram than any other tissue analyzed.*

Phospholipid vesicles, or liposomes, have potential applications in the delivery of biologically active molecules to specific targets in vivo (*1–3*). A variety of substances has been successfully incorporated into liposomes and administered under experimental conditions (*4, 5*). Nevertheless, liposomes have not found widespread use in diagnosis or therapy because they are rapidly cleared from the circulation by the reticuloendothelial system (RES) and concentrated in the liver and spleen (*6*). New *et al.* (*7*) and Alving *et al.* (*8*) applied this phenomenon to treat leishmaniasis in animals. Liposome-entrapped antileishmanial drugs were injected under the assumption that they would concentrate in reticuloendothelial cells, where the parasite proliferates. The encapsulated drugs were approximately 700 times more effective than an equal dose of unencapsulated drugs. Such a method, however, would not allow targeting of liposomes to nonhepatic tissues or malignancies.

Attempts have been made to alter liposome biodistribution by blocking the RES with such substances as carbon, methyl palmitate, latex beads, and dextran sulfate as well as with unlabeled liposomes (*9–13*). The blocking agents were administered before or with labeled

liposomes in order to increase blood levels or alter tissue distribution of the label. These methods were only partially successful in reducing the uptake of liposomes by the spleen and liver, and did not dramatically alter the distribution in other tissues.

Particulate or potentially toxic substances cannot be used clinically to block the RES. However, unlabeled liposomes might be effective as nontoxic, temporary blocking agents. Gregoriadis *et al.* (*14*) attempted to enhance the localization of labeled liposomes in tumors by prior treatment with unlabeled liposomes. While the liver and spleen were partially blocked, the uptake of the label by the tumors was not significantly increased. We report that treatment with unilamellar phospholipid vesicles (diameter, < 0.1 μm) containing a 6-aminomannose derivative of cholesterol (*15*) effectively reduces the subsequent RES clearance of ^{111}In-labeled neutral vesicles and substantially increases tumor-associated radioactivity.

Vesicles containing aminomannose in the lipid bilayer are extremely stable when injected subcutaneously or intravenously (*16–18*). Furthermore, mice injected intravenously with aminomannose-modified vesicles labeled with ^{111}In-nitrilotriacetic acid ([^{111}In]NTA) show a higher concentration of isotope in the liver after 3 hours than mice injected with unlabeled neutral, positive, or negatively charged vesicles (*17*). Also, Wu *et al.* (*19*) showed that phagocytosis of these aminomannose-modified vesicles by mouse peritoneal macrophages proceeds at a high rate in vitro. We previously found that an average of 75 percent of the injected [^{111}In]NTA that is encapsulated in aminomannose-modified vesicles can be recovered in the liver and spleen after 24 hours (*20*). Because this was the highest accumulation of liposome-encapsulated isotope that we had observed in the liver and spleen, we hypothesized that unlabeled aminomannose-modified vesicles would rapidly concentrate in reticuloendothelial cells, temporarily blockading the RES and allowing better nonreticuloendothelial targeting of other types of vesicles.

Cholesterol (CH), distearoyl phosphatidylcholine (DSPC), stearyl amine (SA), and dicetyl phosphate (DCP) were used to prepare vesicles with no charge (DSPC:CH, 2:1 molar ratio), a positive charge (DSPC:CH:SA, 4:1:1), or a negative charge (DSPC:CH:DCP, 4:1:1) (*17, 21*). Aminomannose-modified vesicles were composed of DSPC, CH, and 6-aminomannose (8:3:1). Vesicles were then labeled with [^{111}In]NTA (*21*). Electron microscopy after staining with uranyl acetate showed the mean diameter of neutral vesicles to be 53 nm, compared to 62 nm for positive, negative, and aminomannose-modified vesicles.

Tumors were produced by injecting 5×10^5 EMT6 cells (obtained from R. Klevecz) into the right hind legs of male BALB/c mice (*22*). Ten to twenty days later, tumor-bearing animals were injected with saline or aminomannose-modified vesicles (0.5 to 8 mg in a final volume of 0.5 ml). After 1 hour, [^{111}In]NTA-loaded vesicles (1 to 2 mg) were injected intravenously. The animals were anesthetized and imaged with a gamma camera equipped with a 6-mm pinhole collimator 1 and 24 hours later. Digitized data were stored on magnetic disks for computer analysis. After the second set of images was obtained the animals were killed and dissected to determine the distribution of ^{111}In in their tissues.

Analysis of digitized gamma camera images obtained 1 hour after labeled aminomannose-modified vesicles were injected showed that 80 percent of the injected radioactivity was localized in the liver and spleen (Fig. 1A). This confirms that aminomannose-modified vesicles are rapidly cleared from the blood and suggests that 1 hour might be sufficient to allow for effective blocking of the RES.

Labeled neutral vesicles produced the highest tumor-associated radioactivity of the various vesicle compositions tested (*20*). This effect was not altered by prior treatment with saline (Fig. 1B and Table 1). Mice with 8 mg of nonradioactive

Table 1. Effect of RES blocking with aminomannose-modified vesicles on tissue distribution of ^{111}In 24 hours after intravenous injection. Values are means ± standard errors. *N*, number of animals in that group.

Tissue	Percent of injected dose per gram of tissue for [^{111}In]NTA				
	Unencapsulated ($N = 5$)	In neutral vesicles after saline ($N = 4$)	In neutral vesicles after RES blockade ($N = 5$)	In positive vesicles after saline ($N = 4$)	In positive vesicles after RES blockade ($N = 5$)
Tumor	4.6 ± 1.0	18.5 ± 2.4	28.7 ± 2.6	9.5 ± 1.6	13.3 ± 1.1
Liver	5.4 ± 1.3	14.6 ± 0.8	14.0 ± 2.1	32.7 ± 2.6	25.9 ± 2.9
Spleen	5.0 ± 1.6	18.8 ± 1.6	13.7 ± 1.6	40.6 ± 7.6	38.7 ± 1.6
Blood	0.72 ± 0.16	6.6 ± 0.8	6.8 ± 1.5	1.0 ± 0.2	1.8 ± 0.6
Lung	4.8 ± 2.0	6.0 ± 0.8	6.8 ± 1.5	5.3 ± 0.8	4.7 ± 1.0
Kidney	8.0 ± 0.7	6.8 ± 0.3	6.3 ± 0.7	13.4 ± 2.2	14.0 ± 1.5
Bone	2.7 ± 0.2	3.9 ± 0.8	3.5 ± 1.4	5.0 ± 1.0	4.2 ± 0.6
Muscle	0.72 ± 0.16	1.0 ± 0.3	0.49 ± 0.03	0.84 ± 0.13	0.74 ± 0.08

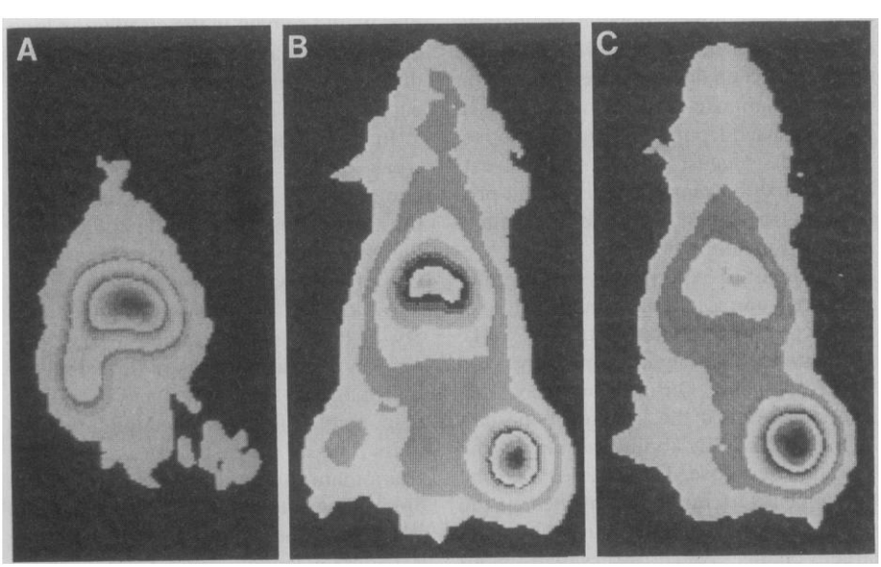

Fig. 1. Digitized whole-body images (dorsal views) of BALB/c mice bearing EMT6 tumors on their right hind legs. (A) One hour after intravenous injection of aminomannose-modified vesicles labeled with [^{111}In]NTA. (B) Twenty-four hours after injection of labeled neutral vesicles; mice were first treated with saline. (C) Twenty-four hours after injection of labeled neutral vesicles; mice were first treated with aminomannose-modified vesicles.

aminomannose-modified vesicles 1 hour before being injected with labeled neutral vesicles consistently showed less radioactivity in the liver and spleen but significantly higher levels of tumor-associated ^{111}In than mice first treated with saline ($P < .005$, Student's t-test) (Fig. 1C and Table 1). The concentration of ^{111}In in the tumors was several times higher than in the blood, indicating that the increased radioactivity was not due to vascular pools in the tumors (Table 1). Also, the accumulation of radioactivity by tumors in mice receiving unencapsulated [^{111}In]NTA (Table 1) was at least three times lower than in mice receiving [^{111}In]NTA-loaded neutral vesicles. Attempts to block the RES by injecting unlabeled neutral vesicles before the administration of [^{111}In]NTA-loaded neutral vesicles decreased the radioactivity in the liver and spleen to 11.0 and 13.8 percent of the injected dose per gram, respectively, but tumor-associated radioactivity remained virtually unchanged at 19.0 percent of the injected dose per gram.

An increase in tumor-associated radioactivity after RES blockade with aminomannose-modified vesicles was also observed when positively charged vesicles labeled with [^{111}In]NTA were the imaging agent (Table 1). However, this procedure produced virtually no change in liver, spleen, or tumor uptake when labeled negative vesicles were given subsequently.

A dose-response relation was observed when groups of animals were treated with increasing doses of aminomannose-modified vesicles before receiving labeled neutral or positive vesicles. Thus tumor-associated radioactivity increased but accumulation in the liver and spleen decreased as the amount of aminomannose-modified vesicles used was increased from 0 to 8 mg per mouse. The results suggest that alternative treatment schedules may be devised that produce better RES blockage and allow even better tumor imaging.

In a separate experiment, treatment of mice with aminomannose-modified vesicles altered the biodistribution of ^{99m}Tc sulfur colloid, an agent commonly used for RES imaging. Our liposome blockade protocol reduced the uptake of the colloid by the liver by about 6 percent of the total injected dose. However, uptake by the spleen was increased by nearly the same amount. Similar, but somewhat larger, changes were observed by Souhami *et al.* (*12*) in studies of the clearance of sheep red blood cells in mice whose RES was blocked with dextran sulfate. Blocking may not affect all the cells of the RES equally, or different mechanisms of clearance may exist for liposomes and larger particles such as colloids or cells.

During the study we observed a relation between tumor size and the amount of associated radioactivity per gram of tumor tissue. Tumors exceeding 0.5 g uniformly accumulated less radioactivity per gram than smaller tumors under identical conditions. Necrotic areas in the larger tumors may be inaccessible to circulating vesicles, resulting in a reduced uptake of ^{111}In. Therefore, the data in this report were pooled from several experiments and represent only those animals whose tumors weighed less than 0.5 g at the time of death.

These findings suggest that intact liposomes are responsible for delivery of ^{111}In to the tumor mass. The increase in the accumulation of ^{111}In in tumors is proportional to the increase in blood ^{111}In. Mauk and Gamble (*23*) showed that most of the blood-borne ^{111}In remains in intact neutral vesicles after 24 hours. However, the increase in tumor-associated ^{111}In after RES blockade cannot be explained merely by the increase in blood-borne radioactivity within the tumor, because distinct tumor images are not observed 1 hour after injection of free or encapsulated [^{111}In]NTA, when the total radioactivity in blood is highest (*17*).

We hypothesize that alterations in capillary permeability or vascular structure, which have been observed in animal (*24, 25*) and human tumors (*26*), allow the smallest liposomes to pass out of circulation and into the tumor. After RES blocking, the loaded neutral vesicles would remain in the circulation longer and thus have a higher probability of diffusing through the permeable tumor capillaries. When the vesicles lyse, the ^{111}In could readily be displaced from the weak chelate, NTA, and form a tight complex with proteins (*27*) fixed in or on the tumor mass, thereby accounting for the progressive and persistent association of ^{111}In with the tumor.

Although EMT6 tumors contain a variety of host cells, including a large proportion of macrophages (*28*), we believe that malignant cells themselves may be responsible for the accumulation of ^{111}In. This is suggested by the fact that aminomannose-modified vesicles did not block, but actually enhanced, uptake of ^{111}In by the tumors. In addition, [^{111}In]NTA-loaded neutral vesicles produced tumor-to-liver specific activity ratios similar to those attained in EMT6 tumor–bearing mice in a variety of histologically distinct murine tumor models, including colon carcinoma 51, mammary adenocarcinoma 16/C, and sarcoma 180.

The results indicate that aminomannose-modified vesicles are effective in blocking the RES. Such blocking may be useful in prolonging the circulation of drugs that are cleared by the RES and could be beneficial in treating rheumatoid arthritis and immune cytopenias, which are RES-dependent. Liposome-induced RES blockage may also provide a novel approach to immunosuppression.

The successful targeting of liposome-encapsulated materials to murine tumors may have even more significance to tumor diagnosis and therapy. If human tumors accumulate liposomes to a similar extent, then labeled vesicles might be useful in determining tumor response to therapy, locating metastases, or even detecting previously undiagnosed tumors. Finally, since many anticancer drugs have been loaded into liposomes (*4*), treatment of tumors that do accumulate ^{111}In-labeled vesicles might be made more effective by subsequently administering vesicles containing an appropriate antineoplastic drug.

RICHARD T. PROFFITT*
Department of Medical Oncology, City of Hope National Medical Center, Duarte, California 91010
LAWRENCE E. WILLIAMS
Department of Radiology, City of Hope National Medical Center
CARY A. PRESANT
Department of Medical Oncology, City of Hope National Medical Center, and *Wilshire Oncology Medical Group, Los Angeles, California 91790*
GEORGE W. TIN
JOSEPH A. ULIANA
RONALD C. GAMBLE
Vestar Research, Inc., Pasadena, California 91106
JOHN D. BALDESCHWIELER
Arthur Amos Noyes Laboratory of Chemical Physics, Department of Chemistry and Chemical Engineering, California Institute of Technology, Pasadena 91125

References and Notes

1. G. Gregoriadis, *N. Engl. J. Med.* **295**, 704 (1976).
2. ———, *Nature (London)* **265**, 407 (1977).
3. B. E. Ryman and D. A. Tyrrell, in *Essays in Biochemistry*, P. N. Campbell and R. D. Marshall, Eds. (Academic Press, London, 1980), p. 49.
4. S. B. Kaye, *Cancer Treat. Rev.* **8**, 27 (1981).
5. M. B. Yatvin and P. I. Lelkes, *Med. Phys.* **9**, 149 (1982).
6. G. Gregoriadis and B. E. Ryman, *Eur. J. Biochem.* **24**, 485 (1972).
7. R. R. C. New, M. L. Chance, S. C. Thomas, W. Peters, *Nature (London)* **272**, 55 (1978).
8. C. R. Alving, E. A. Steck, W. E. Chapman, Jr., V. B. Waits, L. D. Hendricks, G. M. Swartz, Jr., W. L. Hanson, *Proc. Natl. Acad. Sci. U.S.A.* **75**, 2959 (1978).

9. G. Gregoriadis and D. E. Neerunjun, *Eur. J. Biochem.* **47**, 179 (1974).
10. T. Tanaka, K. Taneda, H. Kobayashi, K. Okumura, S. Muramishi, H. Sezaki, *Chem. Pharm. Bull.* **23**, 3069 (1975).
11. V. J. Caride, W. Taylor, J. A. Cramer, A. Gottschalk, *J. Nucl. Med.* **17**, 1067 (1976).
12. R. L. Souhami, H. M. Patel, B. E. Ryman, *Biochim. Biophys. Acta* **674**, 354 (1981).
13. Y. J. Kao and R. L. Juliano, *ibid.* **667**, 453 (1981).
14. G. Gregoriadis, D. E. Neerunjun, R. Hunt, *Life Sci.* **21**, 357 (1977).
15. J. C. Chabala and T. Y. Shen, *Carbohydr. Res.* **67**, 55 (1978).
16. M. R. Mauk, R. C. Gamble, J. D. Baldeschwieler, *Science* **207**, 309 (1980).
17. ———, *Proc. Natl. Acad. Sci. U.S.A.* **77**, 4430 (1980).
18. M. S. Wu, J. C. Robbins, R. L. Bugianesi, M. M. Ponpipom, T. Y. Shen, *Biochim. Biophys. Acta* **674**, 19 (1981).
19. P.-S. Wu, G. W. Tin, J. D. Baldeschwieler, *Proc. Natl. Acad. Sci. U.S.A.* **78**, 2033 (1981).
20. R. T. Proffitt, L. E. Williams, C. A. Presant, G. W. Tin, J. A. Uliana, R. C. Gamble, J. D. Baldeschwieler, *J. Nucl. Med.* **24**, 45 (1983).
21. M. R. Mauk and R. C. Gamble, *Anal. Biochem.* **94**, 302 (1979).
22. S. C. Rockwell, R. F. Kallman, L. F. Fajardo, *J. Natl. Cancer Inst.* **49**, 735 (1973).
23. M. R. Mauk and R. C. Gamble, *Proc. Natl. Acad. Sci. U.S.A.* **76**, 765 (1979).
24. J. C. E. Underwood and I. Carr, *J. Pathol.* **197**, 157 (1972).
25. N. B. Ackerman and P. A. Hechmer, *Surg. Gynecol. Obstet.* **146**, 884 (1978).
26. J. D. Ward, M. G. Hadfield, D. P. Becker, E. T. Lovings, *Cancer* **34**, 1982 (1974).
27. T. K. Leipert, J. D. Baldeschwieler, D. A. Shirley, *Nature (London)* **220**, 907 (1968).
28. D. W. Siemann, E. M. Lord, P. C. Keng, K. T. Wheeler, *Br. J. Cancer* **44**, 100 (1981).
29. We thank M. Miller for electron microscopy. Supported in part by the Clyde and Marian Sluhan Research Fund (L.E.W.), a cancer center seed grant from the City of Hope National Medical Center (R.T.P.), NIH grant GM 21111-09A1 (J.D.B.), NSF grant CHE 81-12589 (J.D.B.), and a grant from the Monsanto Corporation (J.D.B.).
* Present address: Vestar Research, Inc., 939 East Walnut Street, Pasadena, Calif. 91106.

28 October 1982

Hemagglutinin Variants of Reovirus Type 3 Have Altered Central Nervous System Tropism

Abstract. *Variants of the Dearing strain of reovirus type 3 with antigenically altered hemagglutinin proteins are much less neurovirulent than the parental virus. When injected intracerebrally into mice these variants infected a subset of the brain neurons that were infected by the parental virus. When injected intraperitoneally, the variants did not spread to the brain. These results indicate that minor modifications of the reovirus hemagglutinin dramatically alter the ability of the virus to spread into and injure the central nervous system.*

Recent advances in the understanding of genetic and molecular aspects of viral pathogenesis have led to new approaches for studying the basis of recognition of viruses by their receptors (*1*). A striking feature of viral infection is the distribution of virus-induced injury in different tissues. Such distribution may depend in large part on the interaction of viruses with receptors on different subsets of differentiated cells. Thus, although many viruses can interact with the same tissues (for example, the nervous system), differences in the way they interact with such tissues suggest that viruses recognize distinct cell types.

We have used mammalian reoviruses as a model system for studying virus-host interactions and have determined the viral genes responsible for tropism and neurovirulence. We and others showed previously that reovirus type 3 is neurotropic since it infects neurons and causes a diffuse fatal encephalitis (*2, 3*). Reovirus type 1 is not neurotropic since it infects primarily the ependymal cells lining the cerebral ventricles resulting in a nonlethal hydrocephalus (*4*). Genetic studies show that the reovirus hemagglutinin determines the cellular tropism of the reoviruses in the brain (*3, 5*). Thus, the type 1 hemagglutinin interacts with receptors on ependymal cells and the type 3 hemagglutinin binds to receptors on neurons (*1, 6*).

To define the interaction between the reovirus type 3 hemagglutinin and receptors on neurons, we isolated a number of monoclonal antibodies directed to the viral hemagglutinin. By means of these antibodies we showed that there are at least three distinct epitopes on the hemagglutinin, one of which interacts with both neutralizing antibody and cytotoxic T lymphocytes (NT epitope) (*7, 8*). Since this site plays such a central role in determining the specific interaction of reovirus with the immune system, we selected reovirus type 3 variants that were not neutralized by the monoclonal antibodies. These variants induced characteristic cytotoxic T cell responses (*8*) and were less neurovirulent than the parental type 3 virus (*9*).

Here we outline our studies to define the basis for the reduced neurovirulence of the reovirus type 3 variants. We fo-

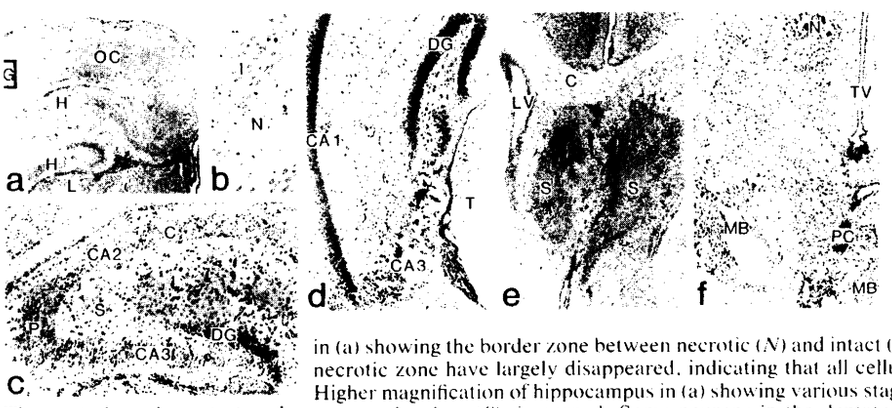

Fig. 1. (a to c) Brain sections from suckling mice injected intracerebrally with the Dearing strain of reovirus type 3. The mice were injected with 10^2 plaque-forming units of virus and killed when moribund. The brains were removed, fixed in Formalin, and sections were stained with hematoxylin and eosin by conventional techniques. (a) Coronal section slightly rostral to the brain level shown in Fig. 2c. The lack of cellular detail in the occipital cortex (*OC*) region and the lateral thalamus (*L*) is indicative of necrosis. Most of the hippocampal gyrus (*H*) is necrotic and cavitated (×33). (b) Higher magnification of region *G* in (a) showing the border zone between necrotic (*N*) and intact (*I*) portions of the occipital cortex. Nuclei in the necrotic zone have largely disappeared, indicating that all cellular types have undergone necrosis (×165). (c) Higher magnification of hippocampus in (a) showing various stages of necrosis cavitation (*C*) in the CA2 region. The central portion, stratum lacunum moleculare (*S*), is normal. Some neurons in the dentate gyrus (*DG*) and CA3 of the hippocampus are pyknotic (*P*), but these regions are relatively spared (×165). (d to f) Brain sections from suckling mice injected intracerebrally with the A variant of Dearing virus. The mice were injected with 10^5 plaque-forming units of virus and killed 15 or 21 days later. Brain sections were prepared as described for (a) to (c). (d) Coronal section at the brain level shown in Fig. 2c. Most of area CA3 of the hippocampus is necrotic and cavitated. The rest of the brain including the dentate gyrus (*DG*) and thalamus (*T*) are normal (×83). (e) Septal area from another mouse showing bilateral necrosis of the septum (*S*). Lateral ventricles (*LV*) are lateral to the septum and the corpus collosum (*C*) is above (×33). (f) Coronal section from the brain in (d) at the brain level shown in Fig. 2b. The rostral portions of the mammillary bodies (*MB*) are bilaterally necrotic and cavitated. There is also a small focus of necrosis (*N*) lateral to the third ventricle (*TV*) (×83). Abbreviations: *AC*, anterior colliculus; *C*, cingulum; *CN*, caudate nucleus; *DG*, dentate gyrus; *DNH*, dorsomedial nucleus of hypothalamus; *H*, hippocampus; *LGB*, lateral geniculate body; *LTN*, lateral thalamic nucleus; *LV*, lateral ventricle; *MB*, mammillary body; *MCN*, medial cuneate nucleus; *MSN*, medial septum nucleus; *OC*, occipital cortex; *S*, subiculum; *SN*, substantia nigra; *STN*, spinal trigeminal nucleus; *TV*, third ventricle; *ZI*, zona incerta.